23rd ABCM International Congress of Mechanical Engineering
December 6-11, 2015, Rio de Janeiro, RJ, Brazil

MODELING THE ACOUSTIC BEHAVIOR OF A LIQUID ROCKET COMBUSTION CHAMBER AT ROOM AND OPERATIONAL CONDITIONS

Pirk, R.[1,2], Souto, C. d´A.[1,2], Araújo, T. B.[1], Almeida, D. S.[1]
Institute of Aeronautics and Space - IAE[1]
Aeronautics Institute of Technology - ITA[2]
e-mails: carloscdas@iae.cta.br, rogeriorp@iae.cta.br, tiagotba@iae.cta.br, danieldsa@iae.cta.br

Abstract. *Combustion instabilities occur when a great amount of energy is concentrated in one or more frequencies, generating pressure peaks much stronger than the background combustion noise. Liquid rocket engines can be affected by low and high frequency instabilities. The latter is related to the interaction of chamber acoustics with combustion process or with propellant injection flow oscillations. Combustion instabilities had been present in the development of liquid rocket engines since the infancy of this technology in the World War II. It can affect the rocket's propulsion system performance even resulting in catastrophic failure and still remains a major design concern. Some researchers pointed out that the combustion does not affect severely the acoustic behavior of a combustion chamber but its acoustic eigenfrequencies (at room temperature) are multiplied by a constant dependent of the operational temperature. In this work the eigenfrequencies of some acoustic modes of a liquid rocket chamber are calculated for room and operational conditions by using analytical methods and the finite element method. A harmonic response analysis is also performed.*

Keywords: *Liquid rocket engine, combustion chamber, combustion instability, acoustic instability, finite element*

1. INTRODUCTION

Over the last years, many rocket motors have experienced the so called phenomenon of the combustion instability [Blomshield, 2001]. This phenomenon severely impairs the operation of both the engine and the vehicle system, and considerable effort has been directed towards solving instability problems. Combustion instability is the interaction of the engine’s inherent pressure/velocity oscillatory modes with the combustion and/or fluid dynamic processes inside the combustion chamber. Through this coupling, the combustion process delivers energy to pressure and velocity oscillations in the combustion chamber. According to Blomshield, 2001, if only a small amount of the available energy (less than one percent) is diverted to an acoustic mode, combustion instability can be generated, yielding ballistic pressure changes and coupling with other components such as guidance or thrust vector control and, in the worst case, cause catastrophic failure. However, combustion instability, although present, sometimes does not cause system problems and can be tolerated in an engine, but it still must be characterized and understood.

Most instability can be classified as being of one of two fundamental types: acoustic-high-frequency or low-frequency. Sometimes, intermediate-frequency, low-amplitude instabilities are distinguished as a third type, to which the term "buzz" has been applied. Buzz instabilities are feed-system combustion and are characterized by wave motion in the chamber at a frequency below that expected for an acoustic chamber mode. As mentioned by Huzel and Huang, 1992, this activity is detected during transients, such as engine start, when chamber acoustic conditions are not well-defined. Figure 1 illustrates an example of detected combustion instabilities.

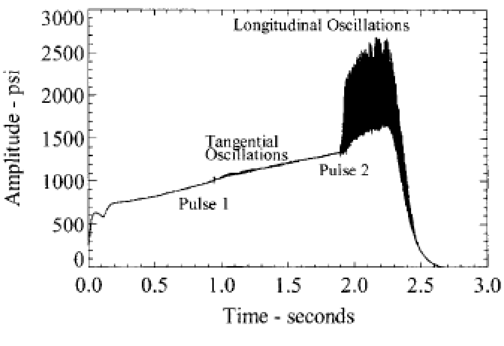

Figure 1: Combustion instabilities (Blomshield, 2001)

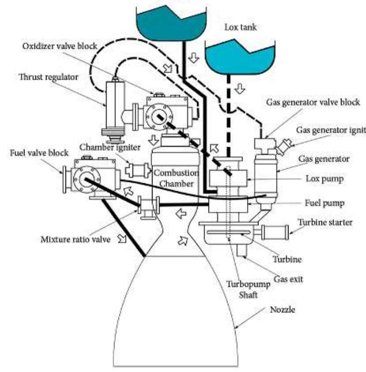

Figure 2: L75 LRPE [Almeida and Pagliuco, 2014]

Acoustic instability is determined by the various acoustic gains and losses in the system. Acoustic gains include coupling between acoustic pressure oscillations and combustion processes, coupling between acoustic velocity and combustion, coupling with burning metal particles away from the propellant surface and flow field interactions (phenomenon like vortex coupling with the motor acoustics). Acoustic loss mechanisms include nozzle damping (acoustic energy lost out through the nozzle), particle damping (for systems with particulates the particles remove acoustic energy), acoustic flow losses (sometimes called flow turning or boundary layer losses), structural damping, and wall losses. Nearly all research in the area of combustion instability is involved in understanding these gains and losses. Elected as a significant issue for the engine's design, the high-frequency or acoustic instability studies must be conducted and the first steps towards these studies may be done by characterizing the internal acoustics of the engine's combustion chamber.

This work focuses only on the acoustic or high-frequency instability, describing the procedures to characterize the internal acoustics of the L75 Liquid Propellant Rocket Engine (LPRE) combustion chamber, seen in Fig. 2. Being developed at Instituto de Aeronáutica e Espaço (IAE), L75 Liquid Propellant Rocket Engine (LPRE) is the first Brazilian open-cycle liquid rocket engine pressurized by turbo pump and designed to deliver 75 kN of thrust in vacuum as a cryogenic upper stage engine using liquid oxygen (Lox) and ethanol (Almeida and Pagliuco, 2014). Firstly, the chamber's ambient or cold-gas acoustic frequencies are analytically calculated, considering a simple equation of the acoustic theory (Natanzon and Culick, 1999, Kinsler et al., 2000 and Laudien et al., 1994). As a second step, the Lox/fuel burning process environment is taken into account and the inherent resonances of the L75 combustion chamber are also determined. The theoretical physical parameters of the burning mix (Lox/ethanol) are used to calculate the sound speed at hot-gas condition and, as a consequence, a scale factor is determined, which is considered to obtain the chamber analytical resonant frequencies shifting at hot-gas conditions.

Finite element numerical calculations are also done, in which finite element models are built aiming at determining the inherent L75 combustion chamber acoustic behavior. The same physical parameters considered in the analytical calculations (for ambient- and hot-gasses conditions) are considered to calculate the inner acoustic modal parameters of the chamber. Numerical vs. analytical results are compared, showing reasonable agreement.

Afterwards, harmonic Frequency Response Analyzes (FRA) are done up to 2,000 Hz and 6,860 Hz, for the ambient- and hot-gasses conditions, respectively. The FE models are submitted to a harmonic excitation and five observation points were generated, on which calculated either the room and hot-gas conditions inner chamber acoustic responses.

Finally, the road map of this research project are described, including the acoustic device treatments to attenuate/suppress pressure oscillations as well as the cold-gas and hot-gas conditions experimental campaigns, planned to be done in the close future.

2. ANALYTICAL AND NUMERICAL ACOUSTIC OSCILLATIONS IN A COMBUSTION CHAMBER

The general features of “vibrations maintained by heat” (as they were called) were firstly understood by the mid-1800s. Rayleigh recognized the crucial phase relationship between the communication of heat and the vibration in a resonator. The classical demonstration consisted of a hydrogen flame burning inside an open tube. Pressure variations in the tube cause the flow of gas, and therefore the heat release, volume expansion, and backpressure on the nozzle to vary during the vibration. This phenomenon is referred to as the "singing flame", which states that if the fluctuating heat release is more in phase than out of phase with the vibration in a resonator, conditions are right for diverting energy into the vibration. Singing flames are analogous to other, more familiar, self-excited vibrations in which the vibrating system extracts its sustaining energy from another system, usually a flowing stream. In a singing flame, combustion provides the energy to sustain gas vibrations inside the combustion chamber.

A steady state is called stable if in a given system any small deviations of the variables from their steady values vanish in the course of the time. In this case, it is assumed that the factors which caused the deviation cease to act after disturbance. On the other side, if in the course of the time the small deviations of the variables defining the system increase spontaneously from their steady values, then the state is called unstable. In such case, soft conditions for loss of stability are referred. Alternatively, hard conditions of the loss of stability apply for sufficiently large disturbances.

Combustion chamber designers have been devoting their studies on suppression/attenuation of pressure oscillations, applying different techniques as baffles, Helmholtz resonators and quarter-wave filters, which produce good results in stabilizing combustion oscillations due to well defined chamber acoustic resonance frequencies. Baffles have been successfully used to prevent transverse acoustic modes of combustion instability and have any effect on feed-system-coupled modes or longitudinal acoustic modes of instability. The transverse modes (tangential and radial) for which baffles have been found effective are characterized by oscillatory pressure waves and gas-particle motion parallel to the propellant injector face. Pressure waves and gas motion affect the combustion processes in a manner such that transient addition to each wave exceeds that wave’s energy losses. The simplest and most widely used approach for the design of baffles is to place them near the gas velocity antinodes of the appropriate chamber acoustic resonance. On the other side, acoustic absorbers as Helmholz resonators and quarter-wave filters have shown to be effective in suppressing acoustic modes of combustion instability in a variety of LRPE (Combs, L. P. et al., 1974). In fact, are currently used either alone or as a supplement to baffles to maintain stable combustion in several engines. A Helmholtz resonator consists of a small passage when the connection of the small cavity volume (the cavity dimensions are small compared with the wavelength) connecting the combustion chamber to a resonator cavity, while a quarter-wave filter is a closed slot or tube (usually straight) with a uniform cross sectional area. This resonator is similar to a Helmholtz resonator except that the cavity dimensions are not compared with a wavelength. In general, these are reactive acoustic devices, where the principle is based on the wave reflection. The traveling waves find an impedance variation (too big or too small) and a small part of the energy is propagated through the silencer, while the other part of the energy is reflected towards the source (Kinsler et al., 2000). However, if any of the attenuation devices is to be applied to acoustic chambers, the design procedure requires the knowledge of the chamber's resonance characteristics, which are usually estimated from the inner acoustics of a combustion chamber.

2.1 Analytical analysis background

The analysis of the acoustics of a closed unbaffled chamber corresponding to the combustion chamber is based on solving the wave equation with appropriate boundary conditions to the chamber configuration. According to Laudien et al., 1994, the combustion chamber and nozzle configuration are treated as a closed/closed system, despite the nozzle is not actually closed. For conventional cylindrical chambers, solutions for simple right cavities with both ends closed and with no through-flow are commonly used. The resonant frequency and locations of maximum amplitude pressure and velocities vary with the acoustic mode. In this way, the tangential and radial (transverse) $\beta_{m,n}$ eigenvalues, the longitudinal eigenvalues *q*, as well as the chamber's geometrical parameters, give the oscillation frequency *f*, in Hz, in a cylindrical chamber as in Eq. (1) (Natanzon and Culick, 1999, Kinsler et al., 2000 and Laudien et al., 1994):

$$f_{m,n,q} = c\sqrt{\left(\frac{\beta_{m,n}}{\phi_c}\right)^2 + \left(\frac{q}{L_c}\right)^2} \quad \text{or} \quad f_{m,n,q} = \frac{c}{2\pi}\sqrt{\frac{\beta_{m,n}{}^2}{R_c{}^2} + \frac{q^2\pi^2}{L_c{}^2}} \tag{1}$$

f: oscillation frequency
c: speed of sound
m, n: tangential and radial mode numbers (0, 1, 2, …)
q: longitudinal eigenvalues (longitudinal mode number), *q* = 1, 2, 3, …
Φc: chamber diameter
Lc: chamber length (replaced by *Le*)
$\beta_{m,n}$: tangential and radial roots of the Bessel function derivative

According to Laudien et al., 1994, the concept of effective length may be adopted in rocket combustion chamber calculations. Therefore, the chamber length *L*c must be replaced by the effective acoustic length (*L*e) aiming at correcting the convergence length of the nozzle throat, since Eq.(1) is formulated for closed cylindrical volumes (Blevins, 1995).

Aiming at calculating the speed of sound to be considered in equations (1), two configurations for the wave propagation inside the acoustic chamber are assumed. Firstly, the ambient (cold-gas condition) temperature was accounted to calculate natural frequencies of the acoustic cavity. Afterwards, the fuel burning process environment inside the chamber was considered and the inherent resonances of this cavity were determined. In hot-gas condition, the global oxidant to fuel ratio (O/F), geometrical constraints and chamber operational pressure are considered to determine the characteristics of the engendered gas due the combustion process. The L75 engine injection head has two different injection zones as: i) outer or peripheral zone where the injectors have lower O/F ratio to reduce the gas temperature close to the engine walls and ii) inner zone or core where the injectors have higher O/F ratio. Due to the required lower temperatures close to the walls, the total chamber mass flow changes from one zone to another, where 61 core injectors are responsible by 80% of the flow, while 30 peripheral injectors are responsible by the remaining 20% of the mass flow. Figure 3 illustrates a schematic drawing of the injection zones distribution, separated by the dotted line.

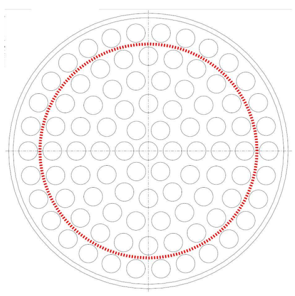

Figure 3: Injection head; outer (or peripheral) and inner (or core) zones

The mass balance from all injectors, considering the mixture of the combustion process, yields a mean O/F ratio of 1.60 for the L75 combustion chamber (Kessaev, J. V., 1997), which is the input data to calculate the gas chemical equilibrium at hot-gas condition by using the NASA-CEA software (Gordon and McBride, 1994, McBride and Gordon, 1996), described in Table 1 (cold-gas condition parameters are described as well). These values are accounted into the calculation of the speed of sound inside the L75 combustion chamber, at cold- and hot-gas conditions, given in Eq. (2) (Kinsler et al., 2000).

$$c = (\gamma RT)^{1/2} \tag{2}$$

where:
γ: ratio of specific heats (*cp/cv*) [no units]
R: specific gas constant [J/(Kg.K)]
T: gas temperature [°K]

Table 1: Parameters for speed of sound calculations

Parameter/Configuration	**Cold-gas (air)**	**Hot-gas (LOx/Ethanol)**
Temperature Celsius [Kelvin]	20.00 [293.00]	3,099.72 [3,372.87]
Mass density ρ [kg/m^3]	1.225	4.77
Molecular mass [g/mol]	28.97	22.88
Specific gas constant R [J/Kg.K]	287.00	363.40
Specific heating at constant pressure cp [J/Kg.K]	1,004	5,498
Ratio of specific heats (cp/cv)	1.4	1.13
Speed of sound c [m/s]	343.11	1,176.87

A few transverse values of the first tangential and radial roots of the Bessel function derivative of the Eq. (1) are given in Tab. 2, which are enough to calculate the chamber natural frequencies up to a significant operational range (Natanzon and Culick, 1999 and Blevins, 1995).

Table 2: First transverse roots of the Bessel derivative $\beta_{m,n}$

m (tangential)	***n (radial)***			
	0	**1**	**2**	**3**
0	0	3.8317	7.0156	10.1730
1	1.8412	5.3314	8.5363	11.7060
2	3.0542	6.7061	9.9695	13.1704
3	4.2012	8.0152	11.3459	14.5859
4	5.3176	9.2824	12.6819	15.9641
5	6.4156	10.5199	13.9872	17.3128

2.2 Finite element analysis background

The FEM (see e.g. Zienkiewicz, 1977, Bathe, 1982 and Hughes, 1987) is the most used numerical technique for solving engineering problems, which consists of finding the distribution of one (or several) field variable(s) in a continuum domain, governed by an appropriate (set of) partial differential equation(s) and boundary conditions.

FEM is based on two concepts:

* transformation of the original problem into an equivalent integral formulation (weighted residual or variational);
* approximation of the field variable distributions and the geometry of the continuum domain in terms of a set of shape functions, which are locally defined within small sub domains (finite elements) of the continuum domain.

Through the application of the element concept, the original problem of determining field variable distributions in a continuum domain is approximately transformed into a problem of determining the field variables at some discrete (nodal) positions within each element. This transformation results in a set of algebraic equations, for which numerical solution procedures are readily available.

The most commonly used finite element implementation for time-harmonic acoustic problems is based on a nodal approximation of the pressure field. The fluid domain V is discretized into a number of finite elements and nodes are defined at some particular locations in each element, usually at the element corner positions. Provided that the finite element discretization (‘mesh’) of the fluid domain V contains a total of n nodes, the acoustic pressure field p in the domain V is approximated as:

$$p(\vec{r}) \approx \sum_{i=1}^{n} N_i(\vec{r}).p_i = [N_i].\{p_i\}. \tag{3}$$

Each function N_i in the *(1xn)* matrix $[N_i]$ is a nodal shape function, associated with node i (i = 1..n). Such a nodal shape function is zero at all node locations in the finite element mesh, except at the location of node i, where it has a unit value. In the domains of those elements, to which node i belongs, the nodal function N_i has a predefined shape, usually based on (low-order) polynomial functions. In the domains of the elements, to which node i doesn't belong, the nodal shape function is identically zero. With this shape function definition, the *(nx1)* vector $\{p_i\}$ comprises the unknown pressure values at each of the node locations.

Based on a weighted residual or variational formulation of the Helmholtz equation (Kinsler et al., 2000), a finite element model in the unknown nodal pressure values p_i is obtained,

$$\left([K_a] + j\omega[C_a] - \omega^2[M_a]\right)\{p_i\} = \{F_a\}. \tag{4}$$

The matrices $[K_a]$ and $[M_a]$ are denoted as, respectively, the acoustic 'stiffness' matrix and the acoustic 'mass' matrix. The acoustic damping matrix $[C_a]$ results from the normal impedance boundary condition. The excitation vector $\{F_a\}$ results from the external acoustic source distribution q and the normal velocity boundary condition. The prescribed pressure boundary condition does not appear explicitly in the finite element model (Desmet and Vandepite, 2001). This boundary condition is taken into account by a priori assigning the prescribed pressure values to the appropriate nodal pressure values and by eliminating these nodal pressures from the vector of unknowns $\{p_i\}$.

Calculation of the undamped acoustic modes

The calculation of the undamped mode shapes of an interior acoustic system, in which the entire boundary surface is assumed to be perfectly rigid, is obtained by discarding the damping matrix $\left[C_a\right]$ and the external excitation vector $\left\{F_a\right\}$ in the FEM. Since the stiffness and mass matrices $\left[K_a\right]$ and $\left[M_a\right]$ are independent of frequency, the mode shape predictions are obtained from the following eigenvalue problem (Desmet and Vandepite, 2001),

$$\left[K_a\right]\left\{\Phi_m\right\} = \omega_m^2.\left[M_a\right]\left\{\Phi_m\right\} \quad (m = 1..n_a) \tag{5}$$

where: each *(n_ax1)* eigenvector $\left\{\Phi_m\right\}$ represents a mode shape and where the associated eigenvalue corresponds to the square of the natural frequency ω_m of that mode.

Note that, due to the discretization of the acoustic system, which has an infinite number of degrees of freedom and, hence, an infinite number of modes, into a system with n_a degrees of freedom, only n_a mode shapes are obtained.

3. ACOUSTIC MODELS OF THE L75 COMBUSTION CHAMBER

3.1 Analytical Model

The L75 combustion chamber geometry, shown in Fig. 3, is accounted to calculate the acoustic analytical natural frequencies of this acoustic cavity. According to Laudien et al., 1994, the concept of effective length may be adopted for rocket combustion chambers, since the geometrical contraction due to the nozzle throat of the chamber must be accounted. Therefore, the chamber length (*L*c) must be replaced by an effective length (*L*e), in Eq. (1), aiming at correcting the convergence length of the nozzle throat. The effective length for longitudinal modes is somewhat less than the actual *L*c because of the gradual contraction in the chamber diameter near the nozzle-throat inlet. In the case of the L75 chamber, a first approximation for *L*e is obtained by accounting the distance between the face plate and nozzle throat less approximately one-third of the convergence nozzle-throat length. In this way, this analytical calculation takes into account the *Lc* = 314.7 mm to obtain the effective length of the chamber (*Le* = 270 mm).

Seven acoustic natural frequencies, associated to the acoustic modes of the L75 combustion chamber are calculated using Eq. (1), up to 2,000 Hz and 6,860 Hz, approximately, for both environmental configurations. Notice that room and burning environment conditions and, consequently, the both speeds of sound described in Tab. 1, are considered in these calculations.

3.2 Numerical model

The acoustic FE model of the L75 combustion chamber was built by using solid elements and accounting the geometry shown in Fig.(3) as well as the room and hot environments parameters (Tab. 1). Aiming at calculating consistent modal data bases for both inner temperature conditions, the cavity mesh was properly discretized. By using at least 8 elements by wavelength for ambient-condition, we can consider that modes until a frequency of 7080 Hz will not be poorly described. This assumption yielded 107445 linear hexahedral elements and 108,632 nodes, for ambient-condition. Figure 4 shows the FE model of the L75 combustion chamber. The chamber acoustic cavity in hot-gas condition presents much higher natural frequencies than in ambient-condition due to the much bigger sound velocity in the hot gas. In order to properly describe modes of higher order to be used in modal superposition, a very fine mesh should be used. However since the mode shapes remains the same and the frequencies are multiplied by a ratio of 3.43, only the cold-gas condition will be analyzed in order to save computational effort. The internal cavity fluid is characterized by the same cold- and hot-gas physical parameters described in Tab. 1 (mass densities and speeds of sound). For both environmental configurations, modal data bases of 650 modes have been calculated.

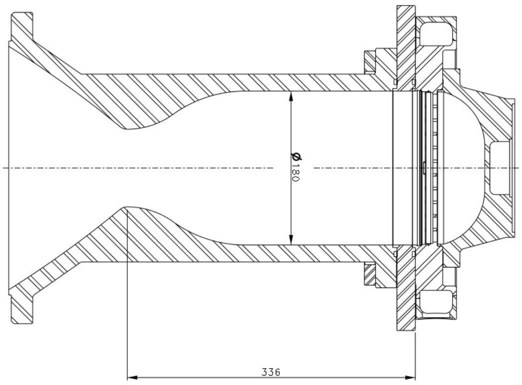

Figure 3: L75 LPRE combustion chamber geometry

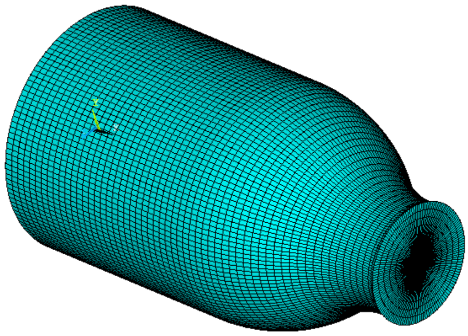

Figure 4: FE model for FRA calculations

The FE model was also used to obtain the internal acoustic response of the combustion chamber. In this framework, harmonic Frequency Response Analyzes (FRA) were done up to 2,000 Hz, in steps of 1 Hz, for the ambient condition. In order to simulate the noise excitation generated during the combustion an unitary velocity was applied to four nodes close to the center of the chamber faceplate. Two observation points, which simulate measurement acoustic microphones, were positioned inside the cavity (central nodes). The modal superposition principle, using the 650 previously calculated modal data basis, was applied to calculate the inner combustion chamber pressure behaviors, either for the room- and hot-gas environmental conditions.

4. RESULTS AND ANALYSIS

Some analytically and numerically calculated frequencies, are described in Tab. 3 either as pure longitudinal, tangential and radial acoustic modes or as combined tangential/radial acoustic modes, for the two environments inside the combustion chamber (cold-gas and hot-gas). Notice in Tab. 3 that the frequencies calculated at hot-gas conditions are scaled from the room-gas conditions at a speed of sound ratio of 3.43 (also assessed in Tab. 1). Figures 5, 6, 7 and 8 show the cold-gas longitudinal, tangential, longitudinal/ tangential and radial modes at 632.63 Hz, 1,146 Hz, 1,407.8 Hz and 2,354 Hz, respectively.

Table 3: Analytical vs. numerical comparisons

Mode description	ambient-gas condition			hot-gas condition		
	Analytical	Numerical	Dif (%)	Analytical	Numerical	Dif (%)
	Frequency (Hz)			Frequency (Hz)		
1st longitudinal	638.23	632.63	0.89	2,189.12	2,169.92	0.89
1st tangential	1,117.16	1,146.00	-2.52	3,831.83	3,930.78	-2.52
2nd longitudinal	1,276,46	1,104.60	15.56	4,378.24	3,788.78	15.56
2nd tangential	1,853.16	1,877.20	-1.28	6,356.28	6,438.80	-1.28
3rd longitudinal	1,914.70	1,574.40	21.61	6,567.36	5,400.19	21.61
1st radial	2,324.91	2353.70	-1.22	7,974.38	8,073.2	-1.22
3rd tangential	2,549.11	2570.90	-0.85	8,743.37	8,818.2	-0.85

Dif=Difference

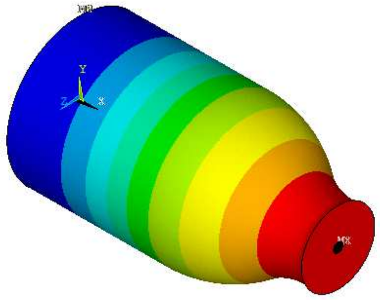

Figure 5: Longitudinal mode (632.63 Hz)

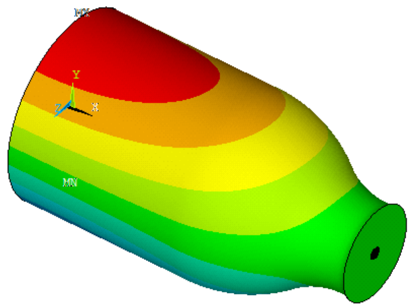

Figure 6: Tangential mode (1,146 Hz)

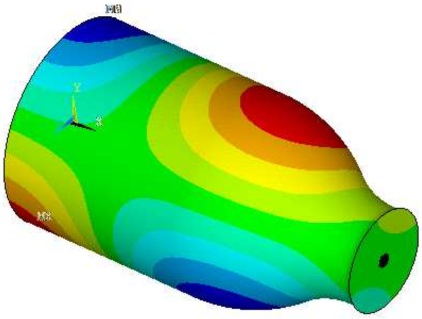

Figure 7: Longitudinal/Tangential mode (1,407.8 Hz)

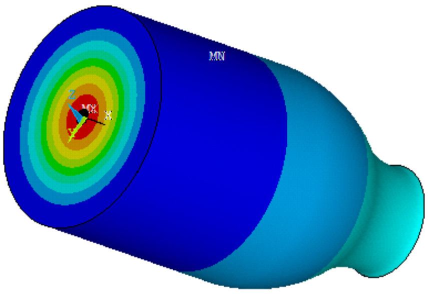

Figure 8: Radial mode (2,354 Hz)

The inner chamber acoustic responses, calculated in the harmonic Frequency Response Analysis (FRA) are shown in Fig.(9), for either ambient and hot internal chamber conditions. The responses at the two observation points are calculated with (virtual) microphones positioned closed to the center of the face plate and at the throat wall, respectively.

Chamber at room temperature
(20^{o} C)

Chamber at operational temperature
(3,100^{o} C)

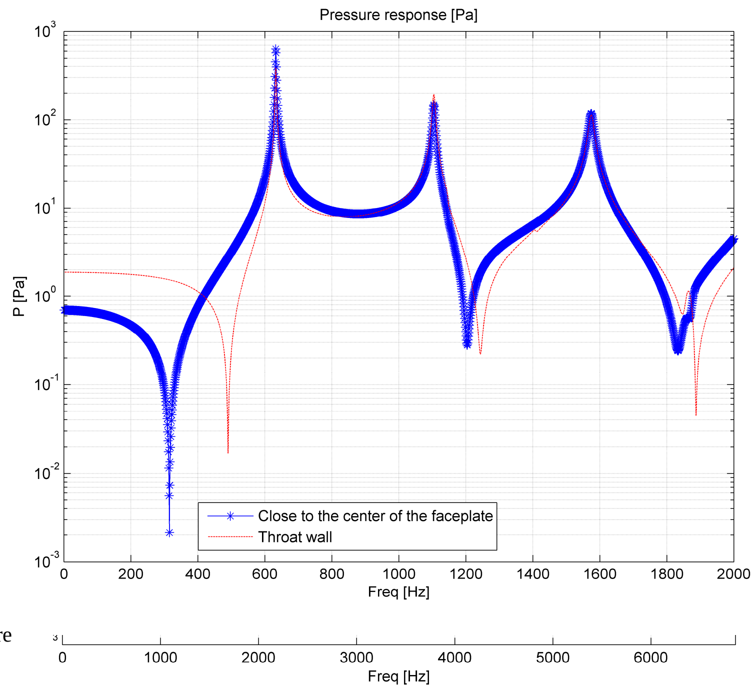

Figure 9: Acoustic responses inside the combustion chamber

5. CONCLUSIONS AND ROAD MAP FOR THE FUTURE

The acoustic dynamic behavior of a combustion chamber was analyzed analytically and numerically by using the finite element method in ambient and hot conditions. The analytical and numerical results showed good agreement for all first seven frequencies but the 2nd and 3rd longitudinal modes. This could indicate that the value of the assumed equivalent length should be re-estimated.

Since the mode shapes remains the same and the natural frequencies is just shifted by the same ratio of the speed of sound in hot/ambient conditions a single run can be used to produce results for both conditions.

In future works, test campaigns with ambient and burning conditions using a L75 engine capacitive combustion chamber shall be done. The internal pressure oscillation measurements results will be used to validate the analytical and numerical models.

6. REFERENCES

Almeida, D. S. and Pagliuco, C. M. M., Development Status of L75: A Brazilian Liquid Propellant Rocket Engine, *Journal of Aerospace Technology and Management, JATM, Vol.6, No 4, pp.475-484, Oct.-Dec., 2014*

Bathe, K-J., *Finite Element Procedures in Engineering Analysis* (Prentice Hall, Englewood Cliffs, New Jersey, 1982).

Blevins, R. D., Formulas for Natural Frequency and Mode Shape, *1st ed., Krieger Publishing Company, USA, 1995.*

Blomshield, F. S., Historical Perspective of Combustion Instability In Motors: Case Studies*, *AIAA/ASME/SAE/ASEE Joint Propulsion Conference and Exhibit, July 8-11, 2001 Salt Lake City, Utah, American Institute of Aeronautics & Astronautics.*

Combs, L. P., Oberg, C. L., Evers W. H. Jr., Liquid Rocket Engine Combustion Stabilization Devices, *NASA SP 8113, November 1974.*

Desmet, W., Vandepite D., *Notes of the Grasmech Course Advanced Acoustics, Finite Elements On Acoustics, Katholieke Universiteit Leuven (KUL),* 2001.

Hughes, T.J.R., *The Finite Element Method : Linear Static and Dynamic Finite Element Analysis* (Prentice Hall, Englewood Cliffs, New Jersey, 1987).

Kessaev, J. V., Theory and Calculation of liquid-propellant engines, Propellant Liquid Engine Course, Technological Institue of Aeronautics - ITA, 1997.

Huzel, D. K. and Huang, D. H., Modern Engineering For Design Of Liquid-Propellant Rocket Engines, *American Institute of Aeronautics and Astronautics, Inc., 1992.*

Laudien, E., Pongratz, R., Pierro, R. and Preclick, D., Experimental Procedures Aiding the Design of Acoustic Cavities, DASA- Deutsche Aerospace AG, Liquid Rocket Engine Combustion Instability, *Progress in Astronautics and Aeronautics, 1994, Chapter 14, volume 169.*

Lawrence E. Kinsler, Austin R. Frey, Alan B. Coppens, James V. Sanders, *Fundamentals of Acoustics, 4th Edition, John Wiley and Sons, Inc., 2000.*

Natanzon, M. S. and Culick, F. E. C., Combustion Instability, *Edited by California Institute of Technology, 1999.*

Zienkiewicz, O.C., *The Finite Element Method - Vol. 1: Basic formulation and linear problems* (McGraw-Hill, London, 1977).

Sanford Gordon and Bonnie J. McBride, *Computer Program for Calculation of Complex Chemical Equilibrium Compositions and Applications – I. Analysis,* Cleveland, Ohio. National Aeronautics and Space Administration. 1994. NASA RP1311-Part 1.

Bonnie J. McBride and Sanford Gordon, *Computer Program for Calculation of Complex Chemical Equilibrium Compositions and Applications – II. Users Manual and Program Description,* Cleveland, Ohio. National Aeronautics and Space Administration. 1996. NASA RP1311-Part 2.

7. RESPONSIBILITY NOTICE